Molecular Plant Pathology

MOLECULAR PLANT PATHOLOGY (2010) **11**(4), 479–493 DOI: 10.1111/J.1364-3703.2010.00624.X

Chitin synthase-deficient mutant of *Fusarium oxysporum* elicits tomato plant defence response and protects against wild-type infection

YOLANDA PAREJA-JAIME[1], MAGDALENA MARTÍN-URDÍROZ[1,†], MARÍA ISABEL GONZÁLEZ RONCERO[1], JOSÉ ANTONIO GONZÁLEZ-REYES[2] AND MARÍA DEL CARMEN RUIZ ROLDÁN[1,*]

[1]*Departamento de Genética, Universidad de Córdoba, Edificio C5, Campus de Rabanales, 14071 Córdoba, Spain*

[2]*Departamento de Biología Celular, Fisiología e Inmunología, Universidad de Córdoba, Edificio C6, Campus de Rabanales, 14071 Córdoba, Spain*

SUMMARY

A mutant of the root pathogen *Fusarium oxysporum* f. sp. *lycopersici*, deficient in class V chitin synthase, has been shown previously to be nonvirulent. In this study, we tested the hypothesis that the cause of its avirulence could be the elicitation of the induced plant defence response, leading to the restriction of fungal infection. Co-inoculation of tomato plants with the wild-type strain and the Δ*chsV* mutant resulted in a significant reduction in symptom development, supporting a protective mechanism exerted by the mutant. The ability of the mutant to penetrate and colonize plant tissues was determined by scanning and transmission electron microscopy, as well as fluorescence microscopy using green fluorescent protein- or cherry fluorescent protein-labelled fungal strains. The extent of wild-type strain colonization in co-inoculated plants decreased steadily throughout the infection process, as shown by the quantification of fungal biomass using real-time polymerase chain reaction. The hypothesis that defence responses are activated by the Δ*chsV* mutant was confirmed by the analysis of plant pathogenesis-related genes using real-time reverse transcriptase-polymerase chain reaction. Tomato plants inoculated with the Δ*chsV* mutant showed a three fold increase in endochitinase activity in comparison with wild-type inoculated plants. Taken together, these results suggest that the perturbation of fungal cell wall biosynthesis results in elicitation of the plant defence response during the infection process.

INTRODUCTION

Fusarium oxysporum is a common soil-borne fungus that causes vascular wilt disease on a wide range of plants, resulting in severe crop losses throughout the world. According to host specificity, *F. oxysporum* isolates have been classified in formae speciales (Armstrong and Armstrong, 1981). As an example, the forma specialis *lycopersici* is pathogenic on tomato plants (*Lycopersicon esculentum*).

Plant infection by pathogenic fungi involves molecular interactions between plants and microbes. In this scenario, the fungal cell wall plays an important role: on the one hand, it provides the necessary rigidity that enables the fungus to enter the plant cells and, on the other, many elicitors are generated from it, alerting the plants to the presence of a potential pathogen and activating the plant defence response. Indeed, it has been reported that the disruption of genes involved in the synthesis and maintenance of the cell wall results in nonvirulent fungal strains (Martin-Urdiroz *et al*., 2008; Soulie *et al*., 2006; Weber *et al*., 2006; Werner *et al*., 2007).

A nonvirulent mutant, Δ*chsV*, affected in cell wall synthesis, has been isolated previously in *F. oxysporum* f. sp. *lycopersici* (Madrid *et al*., 2003). This nonvirulent strain lacks a functional class V chitin synthase, shows an altered cell wall with balloon-like structures along the hyphae and has lost the capacity to infect tomato plants. We proposed that, as a consequence of its altered cell wall, the mutant elicits rapid plant defence responses, leading to host restriction of fungal colonization.

To validate this hypothesis, we performed single- and co-inoculation experiments using the wild-type and/or Δ*chsV* mutant. The results of these experiments were analysed by three approaches. In the first approach, we evaluated disease symptom development in co-inoculated plants. A second approach involved time course analysis of plant colonization by means of visualization of *F. oxysporum* f. sp. *lycopersici*-infected root sections by scanning electron microscopy (SEM), transmission electron microscopy (TEM) and fluorescence microscopy, as well as real-time polymerase chain reaction (PCR) quantification of fungal biomass from each strain within the infected stems. Finally, we analysed whether Δ*chsV* induces plant defence response genes, which may limit the fungal colonization of host

*Correspondence: Email: ge2rurom@uco.es

†*Present address*: School of Biosciences, University of Exeter, Geoffrey Pope Building, Stocker Road, Exeter, Devon EX4 4QD, UK.

tissues and restrict infection by the wild-type strain and nonvirulent mutant, similar to the mechanisms of plant disease control carried out by biocontrol agents (Alabouvette *et al*., 2006; Fravel *et al*., 2002).

RESULTS

Nonvirulent Δ*chsV* mutant protects tomato plants against wilt disease caused by the wild-type strain

To determine whether the nonvirulent mutant Δ*chsV* could protect tomato plants against wilt disease caused by the *F. oxysporum* f. sp. *lycopersici* wild-type strain, co-inoculation was carried out by immersing the roots of 2-week-old tomato plants in microconidial suspensions of the pathogenic wild-type strain and the nonvirulent Δ*chsV* mutant mixed at different ratios. These included the same amount of both strains (5×10^6 wild-type : 5×10^6 Δ*chsV*) and two fold (2.5×10^6 wild-type : 5×10^6 Δ*chsV*) or 10-fold (5×10^5 wild-type : 5×10^6 Δ*chsV*) more mutant than wild-type strain. Plants were scored for vascular wilt symptoms at different time intervals after inoculation. The severity of wilt symptoms in plants inoculated with the wild-type strain alone, at 5×10^6, 2.5×10^6 or 5×10^5 microconidia/mL, increased steadily throughout the experiment, and most plants were dead 25 days after inoculation (data not shown). In contrast, a delay in the development of disease symptoms was observed in plants co-inoculated with inoculum ratios containing at least double the amount of mutant versus wild-type strain. The most significant reduction in the disease index was observed at the ratio 0.1 × wild-type : 1 × Δ*chsV* (5×10^5 : 5×10^6 microconidia/mL, respectively) (Fig. 1a). To demonstrate that the reduction in disease progression during co-infection was not a result of physical competition during attachment to the roots, we performed successive inoculation assays in which tomato roots were first immersed in a microconidial suspension of the wild-type strain (5×10^5 microconidia/mL for 15 min) and subsequently of the Δ*chsV* mutant (5×10^6 microconidia/mL for 15 min). In this way, the wild-type strain was allowed to adhere to the roots without physical interference from the nonvirulent mutant. The results obtained did not differ from those observed during simultaneous co-inoculation using strains at a ratio of 0.1 × wild-type : 1 × Δ*chsV* for 30 min (5×10^5 : 5×10^6 microconidia/mL, respectively). (Fig. 1a). In addition, no differences in the severity of wilt symptoms were found using wild-type inoculum at 0.1 × concentration (5×10^5 microconidia/mL) for 15 min or 1 × concentration (5×10^6 microconidia/mL) for 30 min (data not shown).

To test whether this protective effect was specific for the Δ*chsV* mutant, tomato plants were co-inoculated with the wild-type microconidia and either the nonvirulent Δ*fmk1* mutant (lacking a

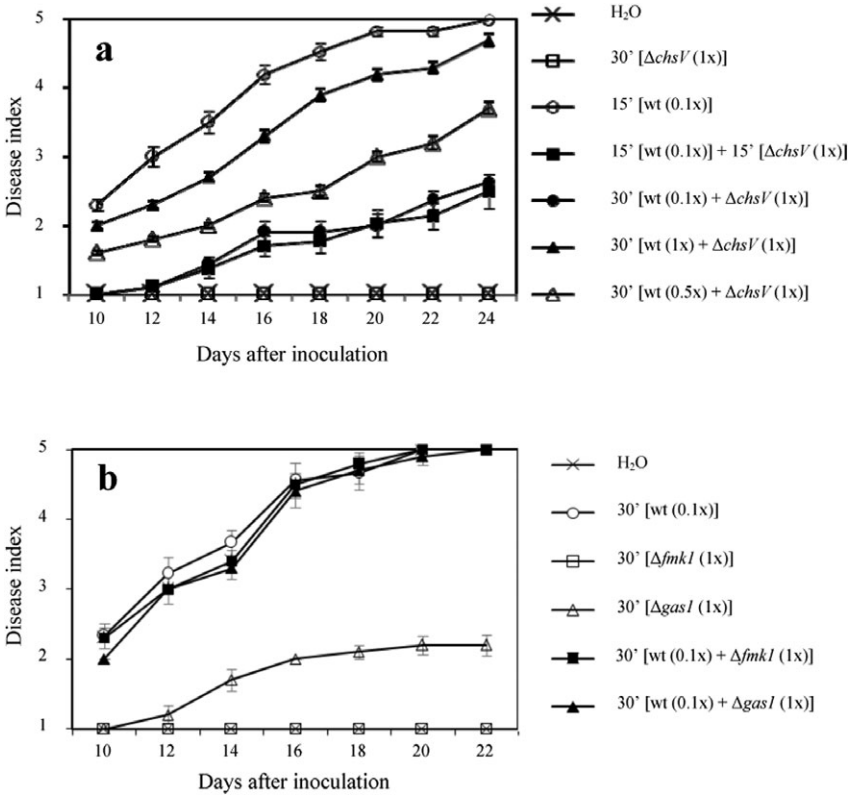

Fig. 1 (a) Progression of wilt symptoms in tomato plants inoculated with the wild-type strain, the Δ*chsV* mutant or simultaneously with both strains in different conditions. The severity of disease symptoms was recorded at different times after inoculation, using an index ranging from 1 (healthy plant) to 5 (dead plant). (b) Progression of wilt symptoms in tomato plants singly inoculated with the wild-type strain, the Δ*gas1* mutant or the Δ*fmk1* mutant, or co-inoculated as indicated. Error bars indicate the standard deviations from three independent experiments, each including 15 plants per treatment. See Table 1 for statistical analysis of the data.

Table 1 Severity of wilt disease in tomato plants inoculated with different combinations of *Fusarium oxysporum* f. sp. *lycopersici* strains.

	Days post-inoculation							
Treatment	10	12	14	16	18	20	22	24
H_2O	1.0 (±0.0) A	1.0 (±0.0) A	1.0 (±0.0) A	1.0 (±0.0) A	1.0 (±0.0) A	1.0 (±0.0) A	1.0 (±0.0) A	1.0 (±0.0) A
30′[Δ*chsV* (1×)]*	1.0 (±0.0) A	1.0 (±0.0) A	1.0 (±0.0) A	1.0 (±0.0) A	1.0 (±0.0) A	1.0 (±0.0) A	1.0 (±0.0) A	1.0 (±0.0) A
15′[wt (0.1×)]†	2.3 (±0.1) B	3.0 (±0.1) B	3.5 (±0.2) B	4.2 (±0.1) B	4.5 (±0.1) B	4.8 (±0.1) B	4.8 (±0.1) B	5.0 (±0.0) B
15′[wt (0.1×)]† + 15′[Δ*chsV* (1×)]*	1.0 (±0.0) A	1.1 (±0.1) A	1.4 (±0.1) C	1.7 (±0.2) C	1.8 (±0.2) C	2.0 (±0.2) C	2.1 (±0.2) C	2.5 (±0.2) C
30′[wt (0.1×)† + Δ*chsV* (1×)*]	1.0 (±0.0) A	1.1 (±0.1) A	1.4 (±0.1) C	1.9 (±0.2) C	1.9 (±0.2) C	2.0 (±0.2) C	2.4 (±0.1) C	2.6 (±0.1) C
30′[wt (1×)† + Δ*chsV* (1×)*]	2.0 (±0.1) B	2.3 (±0.1) C	2.7 (±0.1) D	3.3 (±0.1) D	3.9 (±0.1) D	4.2 (±0.1) D	4.3 (±0.1) D	4.7 (±0.1) B
30′[wt (0.5×)‡ + Δ*chsV* (1×)*]	1.6 (±0.0) C	1.8 (±0.0) D	2.0 (±0.0) C	2.4 (±0.1) E	2.5 (±0.1) E	3.0 (±0.1) E	3.2 (±0.1) E	3.7 (±0.1) D
30′[wt (0.1×)]†	2.3 (±0.2) B	3.1 (±0.2) B	3.6 (±0.2) B	4.5 (±0.2) B	4.7 (±0.2) B	5.0 (±0.0) B	5.0 (±0.0) B	5.0 (±0.0) B
30′[Δ*gas1* (1×)]*	1.0 (±0.0) A	1.2 (±0.1) A	1.7 (±0.2) C	2.0 (±0.0) C	2.1 (±0.1) C	2.2 (±0.1) C	2.2 (±0.1) C	2.2 (±0.1) C
30′[Δ*fmk1* (1×)]*	1.0 (±0.0) A	1.0 (±0.0) A	1.0 (±0.0) A	1.0 (±0.0) A	1.0 (±0.0) A	1.0 (±0.0) A	1.0 (±0.0) A	1.0 (±0.0) A
30′[wt (0.1×)† + Δ*gas1* (1×)*]	2.0 (±0.0) B	3.0 (±0.0) B	3.3 (±0.2) B	4.4 (±0.2) B	4.7 (±0.1) B	4.9 (±0.1) B	5.0 (±0.0) B	5.0 (±0.0) B
30′[wt (0.1×)† + Δ*fmk1* (1×)*]	2.3 (±0.2) B	3.0 (±0.2) B	3.4 (±0.2) B	4.5 (±0.2) B	4.8 (±0.1) B	5.0 (±0.0) B	5.0 (±0.0) B	5.0 (±0.0) B

Values are means (±standard error) for three independent experiments, each including 15 plants per treatment. Means with the same letter within the same column are not significantly different (Duncan, $P \leq 0.05$).

*Concentration 1× corresponds to 5×10^6 microconidia/mL.

†Concentration 0.1× corresponds to 5×10^5 microconidia/mL.

‡Concentration 0.5× corresponds to 2.5×10^6 microconidia/mL.

functional mitogen-activated protein kinase) (Di Pietro *et al*., 2001) or the highly virulence-reduced Δ*gas1* mutant (lacking a functional β-1,3-glucanosyltransferase) (Caracuel *et al*., 2005), which is able to adhere to the root surface and to germinate (Fig. S1, see Supporting Information), using the ratio 0.1 × wild-type : 1 × mutant strain ($5 \times 10^5 : 5 \times 10^6$ microconidia/mL, respectively). No delay in disease development was observed with any of these mutants (Fig. 1b), confirming the specificity of the protective effect exerted by the Δ*chsV* mutant. Significant differences among treatments were confirmed by analyses of variance (ANOVAs) of the data (Table 1).

To rule out a plant genotype effect, simultaneous co-inoculations using strains at the ratio of 0.1 × wild-type : 1 × Δ*chsV* ($5 \times 10^5 : 5 \times 10^6$ microconidia/mL, respectively) for 30 min were performed in three different tomato cultivars, Abramo, Moneymaker and Vemar, all susceptible to *F. oxysporum* f. sp. *lycopersici* wild-type strain 4287 (race 2). In all cases, the results were similar to those observed with cultivar Monika (data not shown).

The Δ*chsV* mutant is able to penetrate and colonize tomato plant tissues

The ability of the Δ*chsV* mutant to adhere to the root surface and to penetrate and colonize the root tissues was compared with that of the wild-type and the nonvirulent mutant Δ*chsV* using light microscopy, SEM and TEM of root sections from infected plants. Light microscopy revealed that, immediately after inoculation, the conidia of the wild-type and the nonvirulent mutant strains became attached to the roots (data not shown). Eight hours after inoculation, they had germinated and started to colonize the root surface (Fig. 2a,e) and, 16 h after inoculation (Fig. 2b,f), hyphae were forming a network interwoven with the root hairs. SEM analysis of infected roots 24 h post-inoculation revealed that, after attachment and germination, both strains formed a dense network randomly distributed around the root surface (Fig. 2c,g). In addition, the nonvirulent Δ*chsV* strain showed swollen structures in subapical regions (Fig. 2g). Although *F. oxysporum* does not produce specialized infection structures, we identified short hyphae penetrating the epidermal cells of the roots during the infection process of both the wild-type and nonvirulent mutant (Fig. 2d,h). TEM analysis showed that, during the first 24 h of infection, hyphae from both the wild-type and nonvirulent mutant penetrated the epidermis and invaded the cortex and the xylem bundles of tip and middle root (Fig. 3a,d), growing inter- or intracellularly (Fig. 3b,e). The invading hyphae appeared to be constricted and often formed a septum at the penetration point (Fig. 3c,f). No structural barriers, such as cell wall appositions, to stop fungal penetration into the root cells were detected during infection with either strain. Likewise, no differences in the accumulation of hydrogen peroxide were observed among plants inoculated with either strain (data not shown).

To follow the colonization process by the wild-type strain and the Δ*chsV* mutant, and to detect possible interactions during co-infection, strains harbouring histone H1 tagged with green fluorescent protein (GFP) or the monomeric cherry red variant (ChFP) of monomeric red fluorescent protein (mRFP), respectively, were used (M. C. Ruiz-Roldán *et al*., unpublished). Inoculation of tomato roots separately (concentration, 5×10^6 microconidia/mL) or simultaneously at a ratio of 0.1 × wild-type : 1 × Δ*chsV* ($5 \times 10^5 : 5 \times 10^6$ microconidia/mL, respectively)

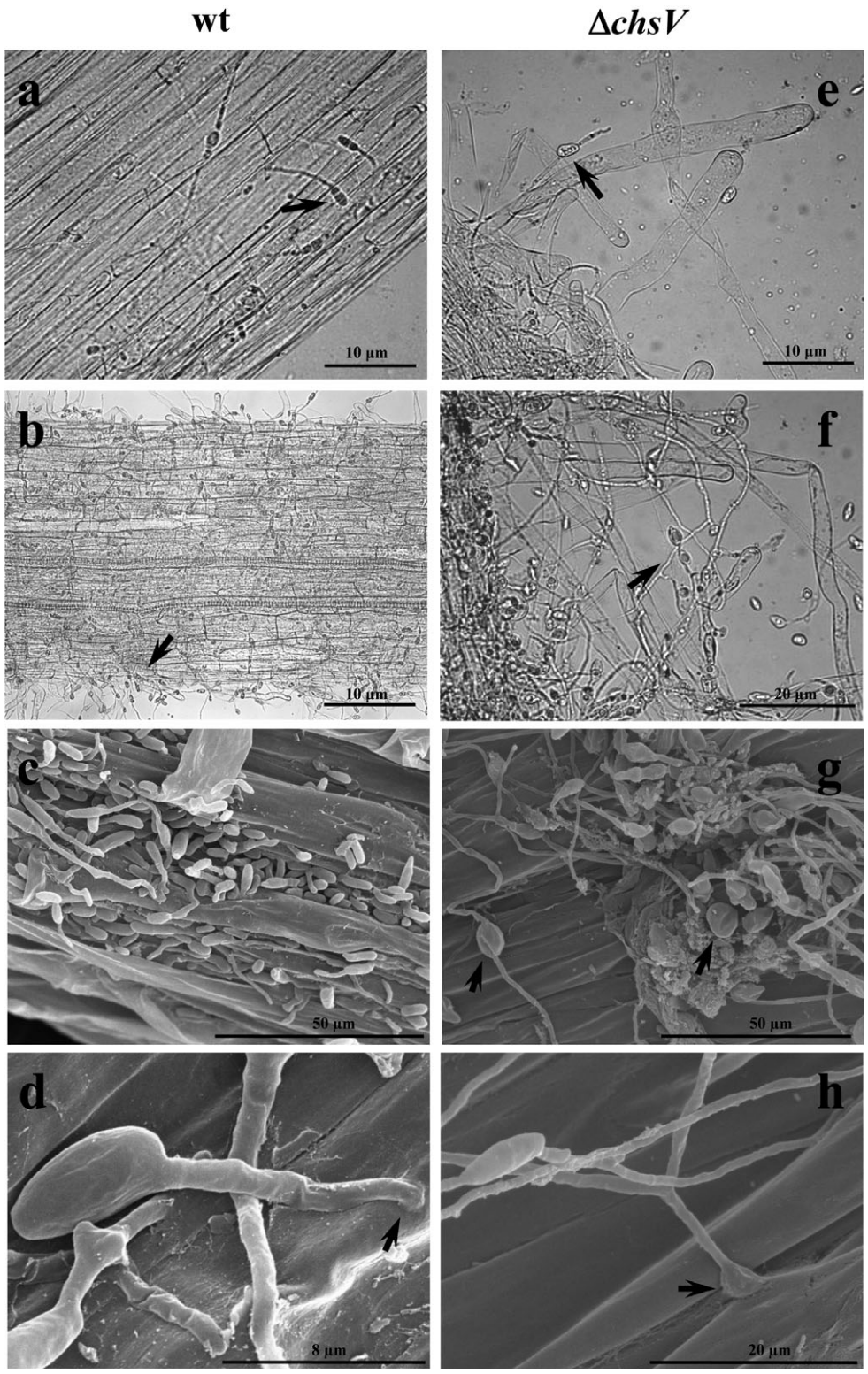

Fig. 2 (a, b, e, f) Light microscopy analysis of tomato roots infected with the wild-type strain (a, b) or the nonvirulent mutant Δ*chsV* (e, f). Micrographs were taken 8 h (a, e) or 16 h (b, f) after inoculation. Arrows indicate germlings adhering to the root surface. (c, d, g, h) Scanning electron microscopy analysis of tomato roots infected with the wild-type strain (c, d) or the nonvirulent mutant Δ*chsV* (g, h). Micrographs were taken 24 h after inoculation. Arrows indicate penetration sites into the root (d, h) and globular structures in the Δ*chsV* mutant (g).

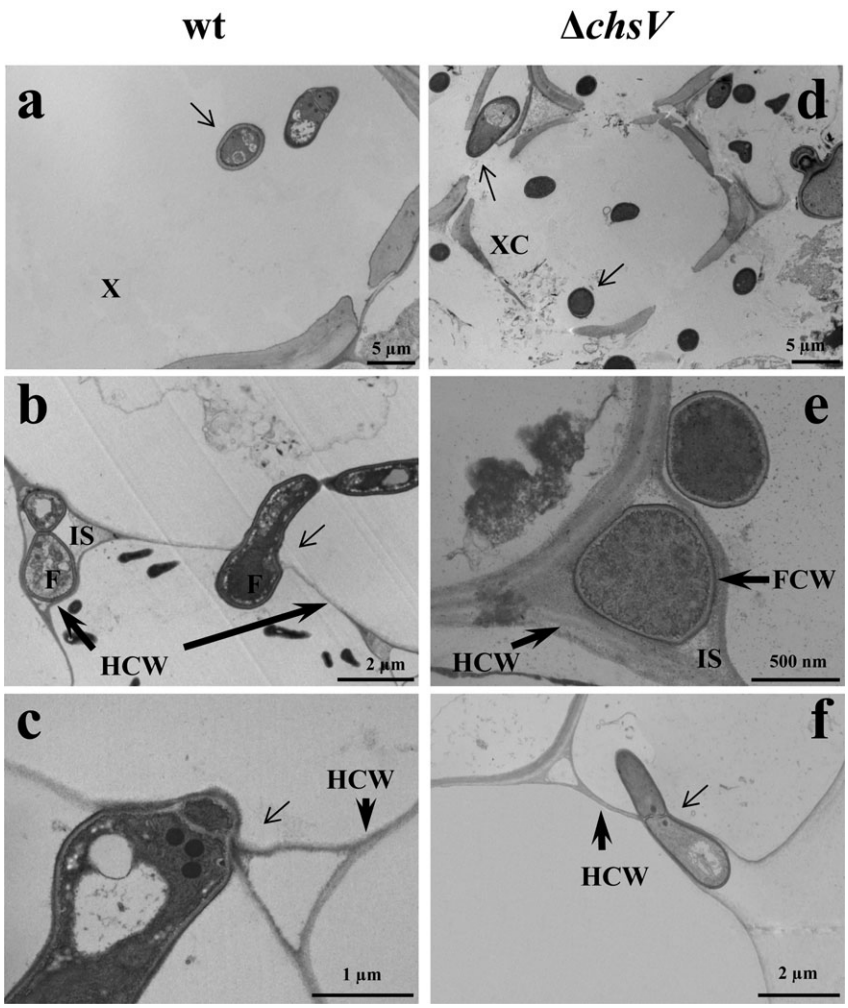

Fig. 3 Transmission electron micrographs of tomato roots inoculated with the wild-type strain (a–c) or the nonvirulent mutant Δ*chsV* (d–f). Micrographs were taken 24 h after inoculation. F, fungal cell; FCW, fungal cell wall; HCW, host cell wall; IS, intercellular space; XC, xylem cell. Thin arrows indicate fungal cells (a, d) or cell penetration sites (b, c, f).

was carried out, and sections of infected roots were observed under a microscope using the differential interference contrast (DIC) technique or fluorescence. The presence of green- or red-labelled nuclei in single-inoculated plants confirmed the colonization of root tissues by both the virulent and nonvirulent strains, respectively (Fig. S2, see Supporting Information). Colonization was massive in infected plants, where labelled nuclei were visualized in all root tissues (Fig. S2c,d). Micrographs obtained using DIC from the infected root sections showed no externally attached hyphae (Fig. S2a,b), leading to the conclusion that the fluorescence-tagged nuclei observed corresponded to mycelium growing inside the plant tissues.

After co-inoculation of tomato roots with both strains at a ratio of 0.1 × wild-type : 1 × Δ*chsV* ($5 \times 10^5 : 5 \times 10^6$ microconidia/mL, respectively), we observed fluorescence-tagged nuclei from both strains in the infected roots (Fig. 4). Although the inoculum density of the nonvirulent mutant was 10-fold higher than that of the wild-type strain, the extent of colonization by the two strains appeared to be similar, at least at the spatial root level analysed in this study. Considering that the observation of fluorescence nuclei is only a qualitative method, it should not be interpreted for the quantification of plant colonization by any of the strains.

Δ*chsV* mutant restricts colonization of tomato plant tissues by *F. oxysporum* wild-type strain

The estimation of the wild-type or Δ*chsV* biomass growing inside the infected plants was performed by quantification of specific fungal DNA within stems using real-time PCR. The amount of fungal biomass in the stems increased during the course of infection in wild-type inoculated plants, with maximal levels at 5 and 7 days after inoculation (Fig. 5a). By contrast, very low levels of wild-type strain were detected in co-inoculated plants (Fig. 5a). However, no significant differences in the amount of DNA amplified from Δ*chsV* were observed between single and co-inoculated plants (Fig. 5b) at any time point. The total amount of mutant genomic DNA decreased during the course of infec-

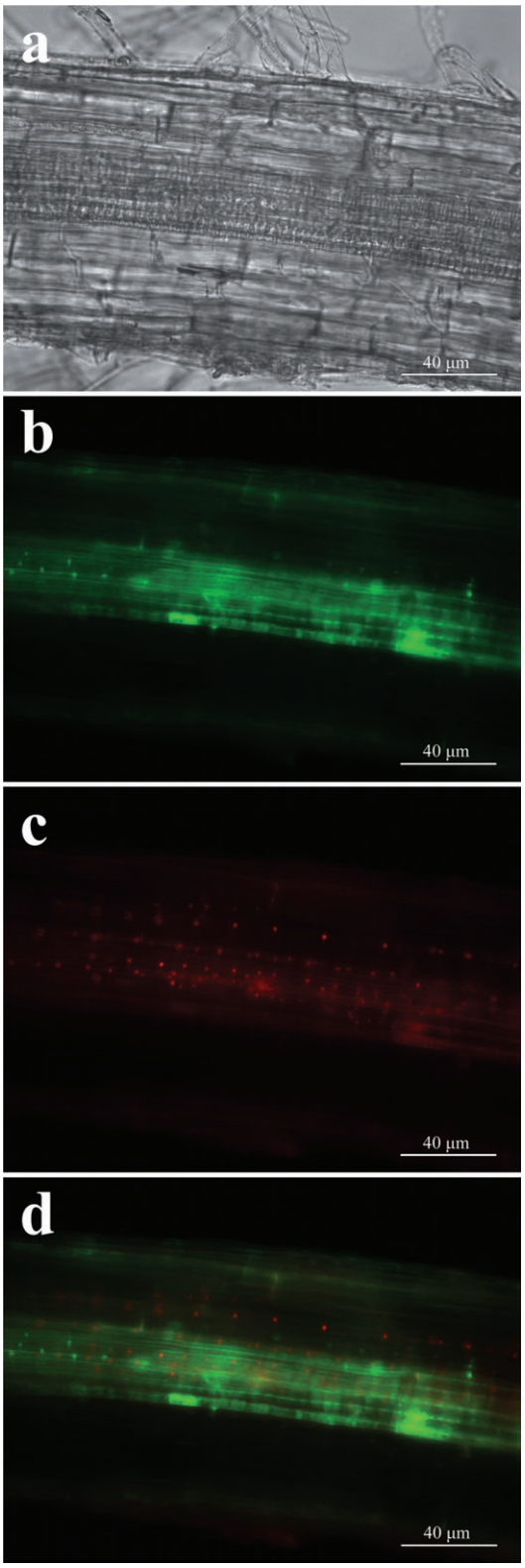

Fig. 4 Co-localization of wild-type strain [harbouring green fluorescent protein (GFP)-tagged H1 histone, green] and Δ*chsV* mutant [harbouring cherry red fluorescent protein (ChFP)-tagged H1 histone, red] during co-infection of tomato roots. Differential interference contrast (a) and fluorescence (b, c) micrographs were taken 5 days after co-inoculation with the wild-type strain and the Δ*chsV* mutant in the ratio $5 \times 10^5 : 5 \times 10^6$ microconidia/mL, respectively (0.1× : 1×). (d) Images (b) and (c) merged.

tion, with a peak at 3 days after inoculation. Larger amounts of Δ*chsV* genomic DNA were detected compared with genomic DNA of the wild-type strain (Fig. 5a,b), probably as a result of the different inoculum concentrations used (5×10^5 microconidia/mL for the wild-type strain, and 5×10^6 microconidia/mL for the Δ*chsV* mutant). To avoid differences caused by inoculum concentration and primer efficiencies, quantitative real-time PCR experiments were performed on plants inoculated with either the wild-type strain or the Δ*chsV* mutant at 5×10^6 microconidia/mL, using a primer pair corresponding to the *F. oxysporum actin1* gene (Table S2, see Supporting Information). At 3 days after inoculation, the amount of fungal DNA in the stems of plants inoculated with the Δ*chsV* mutant was significantly higher than that in those inoculated with the same number of spores of the wild-type strain (Fig. 5c). By contrast, 7 days after inoculation, the wild-type strain was more abundant than the Δ*chsV* mutant. The apparent discrepancies observed in the amounts of fungal DNA amplified from plants inoculated with the same strain using different primer pairs are probably a result of the different amplification efficiencies of the three primer sets used (Fig. 5). Differences among treatments within each day were confirmed by ANOVAs of the data (Duncan, $P \leq 0.05$). These data suggest that, during the first 3 days of infection, the Δ*chsV* mutant colonizes the stem tissues more efficiently than does the wild-type strain, but then gradually declines.

To test the possibility that the Δ*chsV* mutant inhibits directly the growth of the wild-type strain, we performed *in vitro* fungal inhibition assays by co-inoculation into either liquid or solid minimal medium (Fig. 6). No reduction in wild-type growth was observed, in the number of colony-forming units, distance between colony margins or colony diameter, indicating that the Δ*chsV* mutant did not produce any fungal growth inhibitor.

Cell wall-degrading enzyme (CWDE)-encoding genes are not differentially induced during plant infection

Fungal secreted CWDEs have multiple functions in virulence, including host penetration, nutrient acquisition, pathogen cell wall remodelling and elicitation of the plant defence response (Di Pietro *et al*., 2009). *Fusarium oxysporum* produces a remarkable variety of CWDEs belonging to different glycosyl hydrolase (GH) families, such as pectinases, cellulases and xylanases,

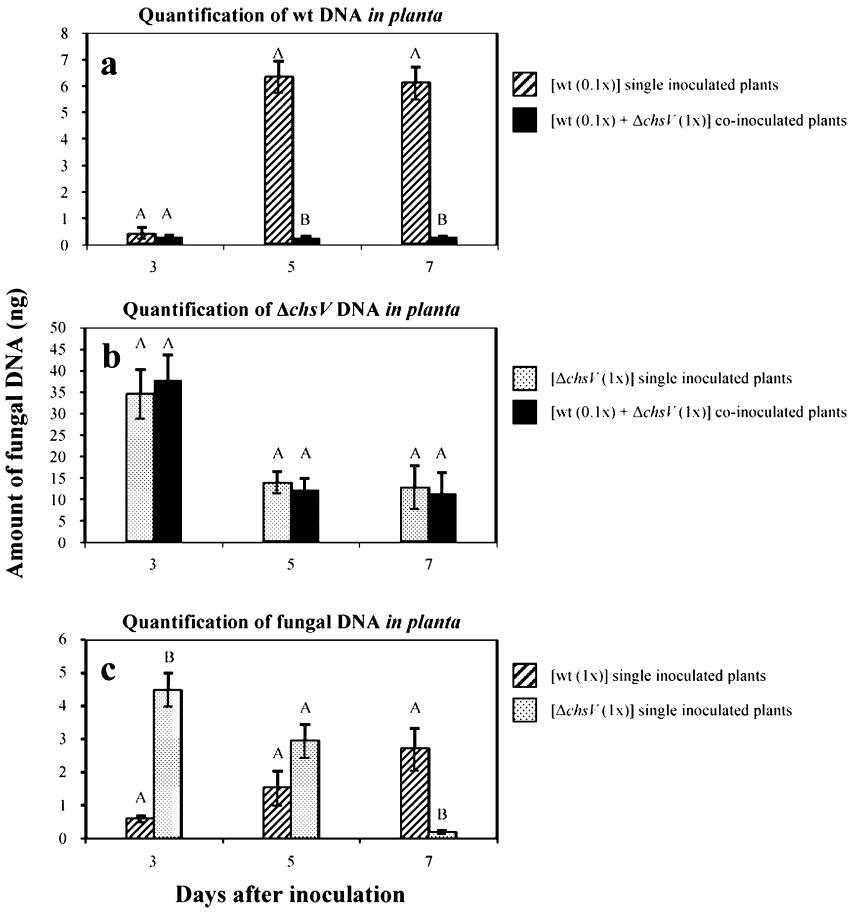

Fig. 5 Comparative analysis of fungal biomass during single- or co-inoculation experiments. (a) Quantitative real-time polymerase chain reaction (PCR), with primer pair CHSV-3 and CHSV-26 specific for the wild-type strain, on total DNA from single-inoculated (striped bars) (using inoculation density of 5×10^5 microconidia/mL) or co-inoculated (black bars) (using the ratio 5×10^5 microconidia/mL wild-type : 5×10^6 microconidia/mL Δ*chsV* mutant) tomato plants. (b) Quantitative real-time PCR, with primer pair GPDA-16 and CHSV-6 specific for the Δ*chsV* mutant, on total DNA from single-inoculated (dotted bars) (using inoculation density of 5×10^6 microconidia/mL) or co-inoculated (black bars) (using the ratio of 5×10^5 microconidia/mL wild-type : 5×10^6 microconidia/mL Δ*chsV* mutant) tomato plants. (c) Quantitative real-time PCR, with a primer pair specific for the *Fusarium oxysporum actin1* gene, on total DNA from plants singly inoculated with the wild-type strain (striped bars) or the Δ*chsV* mutant (dotted bars) using an inoculation density of 5×10^6 microconidia/mL in both cases. Data represent nanograms of fungal DNA amplified from 100 ng of DNA extracted from infected stems. Each column represents the mean from three independent inoculation experiments with three replicates each. Standard error bars are indicated. Columns with the same letter within the same day are not significantly different (Duncan, $P \leq 0.05$).

among others, that are important for degrading plant cell wall components (Di Pietro *et al*., 2003). To test whether GH genes are differentially expressed in the Δ*chsV* mutant and the wild-type strain during the early stages of plant infection, reverse transcriptase (RT)-PCR was performed using RNA isolated from infected tomato roots 3 days after inoculation. The analysis included 21 genes belonging to different GH families, such as β-glucuronidase (GH79), β-1,3-glucanase (GH64), polygalacturonase (GH28) and chitinase (GH18), among others (gene identification numbers are listed in Table S2). No differences in transcript levels were observed in plants inoculated with either strain. The expression of six representative genes is depicted in Fig. S3 (see Supporting Information).

Plant defence responses are differentially activated by the Δ*chsV* mutant in single and co-infected tomato plants

The plant defence reaction in response to co-infection with the wild-type and nonvirulent Δ*chsV* strains was analysed by the quantification of transcript levels of defence-related genes encoding extracellular invertase (*lin6*) (Hedley *et al*., 1994), acidic (*gluA*) and basic (*gluB*) glucanases (van Kan *et al*., 1992), acidic chitinase 3 (*chi3*), basic chitinase 9 (*chi9*) (Danhash *et al*., 1993) and pathogenesis-related protein 1 (*pr-1*) (van Kan *et al*., 1992) in tomato plant roots at 24 h post-inoculation, using quantitative real-time RT-PCR (Fig. 7a). The expression level of

a

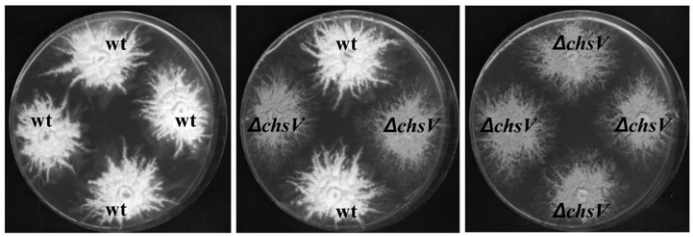

b

	0 h	2 h	4 h	6 h	8 h
wt (single inoculation)	1.18 ± 0.10	1.02 ± 0.03	1.05 ± 0.10	0.94 ± 0.05	1.06 ± 0.09
wt (co-inoculation)	1.21 ± 0.03	1.03 ± 0.09	1.07 ± 0.22	0.96 ± 0.08	1.04 ± 0.04
Δ*chsV* (single inoculation)	1.54 ± 0.01	1.47 ± 0.04	1.51 ± 0.12	1.62 ± 0.10	1.79 ± 0.05
Δ*chsV* (co-inoculation)	1.55 ± 0.10	1.55 ± 0.14	1.52 ± 0.21	1.58 ± 0.10	1.82 ± 0.01

Fig. 6 (a) Colony growth of the wild-type strain and the Δ*chsV* mutant in solid minimal medium; 10^3 spores of each strain were inoculated and the plates were incubated at 28 °C for 7 days. (b) Number of colony-forming units/mL ($\times 10^5$) of the indicated strains after different times of growth on single or co-inoculated liquid cultures.

each defence-related gene was compared among plants infected with either the wild-type strain (at concentrations of 5×10^5 or 5×10^6 microconidia/mL), nonvirulent Δ*chsV* mutant (at 5×10^6 microconidia/mL), or co-inoculated with both strains (5×10^5 microconidia/mL wild-type : 5×10^6 microconidia/mL Δ*chsV*), as well as noninoculated control plants, and referred to the relative levels of the constitutive reference gene *gapdh* encoding the glyceraldehyde-3-phosphate-dehydrogenase (Shih *et al*., 1991). The expression levels of the six genes detected in plants inoculated with the wild-type strain did not differ significantly from those observed in the noninoculated controls (Fig. 7a). By contrast, transcript levels of *lin6*, *gluB*, *chi3*, *chi9* and *pr-1* were significantly higher in plants inoculated with the Δ*chsV* mutant and in co-inoculated plants, compared with plants inoculated with the wild-type strain or the noninoculated controls. In the case of *gluA*, transcription levels were significantly reduced in plants inoculated with the Δ*chsV* mutant, as well as in co-inoculated plants, in comparison with noninoculated controls or plants inoculated with the wild-type strain. Differences in transcript levels among treatments were confirmed by ANOVAs of the data (Duncan, $P \leq 0.05$).

In order to study the persistence of the induced plant defence response, transcript levels of the six defence-related genes were quantified 3, 5 and 7 days after inoculation. The results obtained 3 days after inoculation were similar to those observed 24 h post-inoculation (data not shown) but, after 5 days, the expression levels of *lin6*, *gluB*, *chi3* and *chi9* decreased in plants inoculated with the Δ*chsV* mutant, as well as in co-inoculated plants, whereas the levels of *gluB*, *chi3* and *chi9* increased significantly in plants inoculated with the wild-type strain (Fig. 7b). The expression of *pr-1* increased through time in all treatments, except for the noninoculated controls. The increase ranged from five fold in plants inoculated with the Δ*chsV* mutant, or in co-inoculated plants, to 50-fold in plants inoculated with the wild-type strain (Fig. 7b). Differences in transcript levels among treatments and time points were confirmed by ANOVAs of the data (Duncan, $P \leq 0.05$). The results observed 7 days after inoculation were similar to those obtained 5 days post-inoculation (data not shown).

Chitinase activity is commonly induced as part of the plant defence response (Dalisay and Kuc, 1995; Heath, 1996). A significant increase in endochitinase activity, with a maximum at 3 days post-inoculation, was observed in Δ*chsV* and co-inoculated plants, in comparison with wild-type inoculated plants and the noninoculated controls (Fig. 7c). No significant differences were observed in exochitinase activity. Noninoculated controls showed basal levels of chitinase activity that remained constant throughout the experiment (data not shown). Differences in chitinase activity among treatments were confirmed by ANOVAs of the data (Duncan, $P \leq 0.05$).

DISCUSSION

Colonization of plant tissues by the nonvirulent mutant Δ*chsV*

In order to clarify the molecular basis for the inability of the Δ*chsV* mutant to cause wilt disease on tomato plants, we carried out a comparative microscopy analysis of the infection process of the Δ*chsV* mutant and wild-type strain. We demonstrated that, after adhesion to the root surface, both strains were able to penetrate the epidermal cells and colonize the root tissue. Interestingly, 3 days after inoculation, the amount of fungal biomass detected in the stems of tomato plants inoculated with the Δ*chsV* mutant was significantly higher than that in those inoculated with the wild-type strain, suggesting that the mutant colonizes plant tissues more efficiently than the wild-type strain during the early stages of infection. However, no differences in the growth rate were found between these strains during *in vitro* culture. As shown previously, the absence of ChsV does not

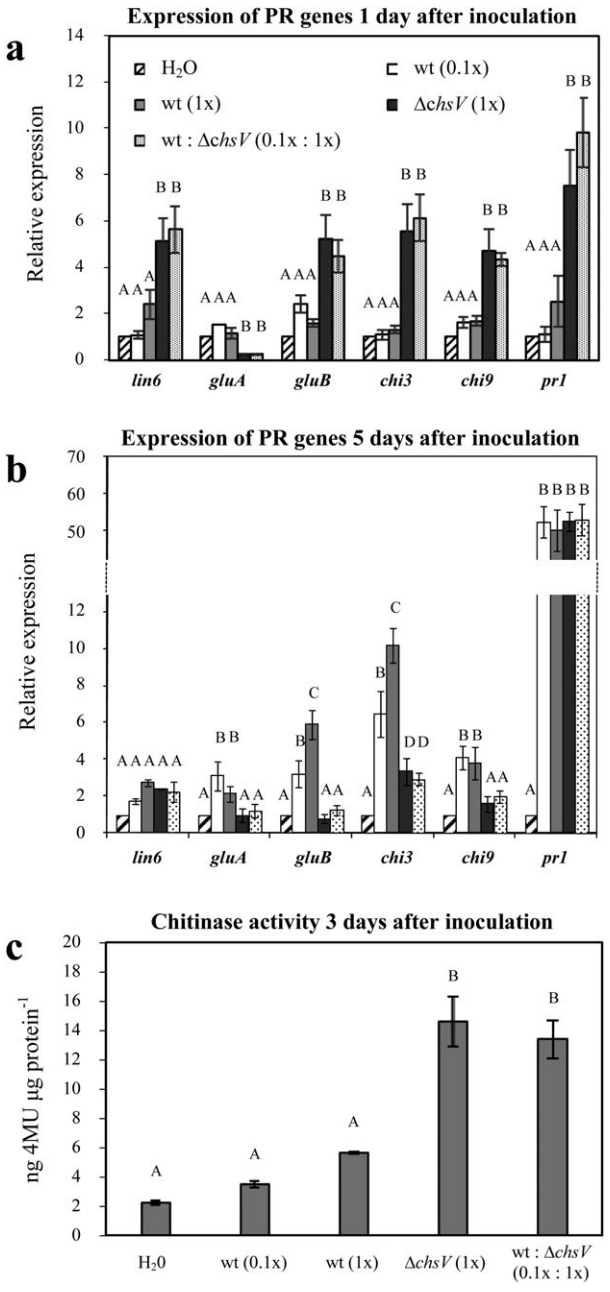

Fig. 7 (a, b) Expression of defence-response genes in tomato plants at 1 (a) or 5 days (b) after inoculation with the wild-type strain at concentrations of 5×10^5 microconidia/mL (white bars) and 5×10^6 microconidia/mL (grey bars), mutant at 5×10^6 microconidia/mL (black bars) or both strains simultaneously in the ratio of 5×10^5 microconidia/mL wild-type : 5×10^6 microconidia/mL Δ*chsV* mutant (dotted bars), and the noninoculated controls (striped bars). Transcript abundance was determined by quantitative reverse transcriptase-polymerase chain reaction. Expression levels in each sample were normalized to the expression of the tomato *gadph* gene and were calculated relative to the uninfected control plants by the ΔΔCt method. Error bars indicate the standard error calculated from four independent inoculation experiments with two replicates each. Columns with the same letter within the same gene are not significantly different (Duncan, $P \leq 0.05$). (c) Endochitinase activity in stems of tomato plants 3 days after inoculation with the indicated strains at the indicated concentrations (0.1×, 5×10^5 microconidia/mL; 1×, 5×10^6 microconidia/mL). Noninoculated plants (H_2O) were used as controls. Chitinase activity is expressed as nanograms of 4-methylumbelliferone (4MU) released from the substrate per microgram of protein. Error bars indicate standard deviations from three independent inoculation experiments. Columns with the same letter are not significantly different (Duncan, $P \leq 0.05$).

induce the expression of the genes involved in fungal cell wall synthesis, such as *chs1*, *chs2*, *chs3*, *chs7*, *gas1* or *rho1* (Caracuel *et al*., 2005; Madrid *et al*., 2003; Martin-Urdiroz *et al*. 2008), which might be subjected to possible compensatory mechanisms. Nevertheless, we do not exclude the existence of unidentified additional traits influencing the rapid and abundant colonization of tomato tissues by the Δ*chsV* mutant.

Our results disagree with previous studies conducted in the Δ*chsV* mutant, where the growth of this strain was not detected inside inoculated plants (Madrid *et al*., 2003). The discrepancy between the two studies could be a result of the different accuracy of the methods used.

Protection against tomato wilt disease by the nonvirulent mutant Δ*chsV*

As a second approach, we explored the hypothesis that the Δ*chsV* mutant colonizes the plant but, as a consequence of its altered cell wall structure, rapidly elicits an intense and effective plant defence response, leading to a restriction of pathogen colonization. If this assumption is correct, the plant should show reduced disease symptoms on infection with the *Fusarium* wild-type strain in the presence of the Δ*chsV* mutant. We performed co-inoculation experiments with both strains and observed a significant delay in the appearance of disease symptoms in co-inoculated plants. This protective effect was only detected with the cell wall-defective mutant Δ*chsV*, as other nonvirulent mutants (Δ*gas1 or* Δ*fmk1*) did not protect against infection by the wild-type strain. It has been shown previously that inoculation with avirulent isolates of *F. oxysporum* can result in a significant reduction in disease symptoms caused by virulent isolates from the same or a different forma specialis (Huertas-Gonzalez *et al*., 1999). However, as most of these strains are soil-borne nonpathogenic isolates, there is insufficient knowledge about the biochemical and genetic bases that differentiate them from the virulent strains and enable them to protect plants against pathogens. Some authors have proposed the use of nonvirulent mutants as biocontrol agents for fungal pathogenesis. A nonvirulent mutant of the ascomycete *Colletotrichum magna* (path-1) was able to colonize cucurbit plants without

inducing disease symptoms, and protected plants against *C. magna*, *F. oxysporum* (Freeman and Rodriguez, 1993) and *C. orbiculare* (Redman *et al*., 1999a). This nonpathogenic mutant is impaired in the production and secretion of pectate lyase and endopolygalacturonase (Wattad *et al*., 1995), and elicits a more rapid, intense and localized defence response (Redman *et al*., 1999a). Likewise, the *C. magna* R1 nonvirulent mutant confers protection to watermelon plants against the wild-type strain (Redman *et al*., 1999b). *Fusarium oxysporum* f. sp. *melonis* nonvirulent mutant 4/4 significantly reduces the mortality of muskmelon and watermelon plants caused by *F. oxysporum* f. sp. *melonis* (race 1,2) and *F. oxysporum* f. sp. *niveum* (race 2), respectively (Freeman *et al*., 2001).

The protective abilities of biocontrol agents generally involve multiple mechanisms expressed successively, simultaneously or synergistically, including microbial antagonism (parasitism, competition for nutrients or for the colonization of plant tissues, and antibiosis) and induced resistance of the plant (reviewed by Alabouvette *et al*., 2009). On the basis of the results of the *in vitro* fungal inhibition assays, we exclude the possibility that Δ*chsV* inhibits the growth of the wild-type strain. However, the fact that protection was increased with a higher inoculum density of the nonvirulent mutant versus the wild-type, together with the small amount of wild-type biomass present in stems of co-inoculated plants, suggest that both strains are competing for nutrients and/or plant tissues. The direct competition between two strains of *F. oxysporum* (nonvirulent and virulent) within the host plant has been proposed previously as the cause of the reduced colonization of the carnation *Dianthus caryophyllus* stem by the pathogenic strain, resulting in a decrease in disease severity (Postma and Luttikholt, 1996).

Activation of the plant defence responses

The induction of tomato defence responses by the Δ*chsV* mutant could also be one of the reasons for the protective effect exerted by this strain. Indeed, expression analysis of plant defence-related genes revealed an earlier accumulation of higher levels of transcripts in plants inoculated with the nonvirulent mutant, in comparison with the wild-type strain and the noninoculated controls, as early as 24 h post-inoculation. This rapid and intense activation of plant defences on infection by the Δ*chsV* mutant, together with the higher sensitivity of this mutant to plant defence compounds, would lead to an efficient restriction of fungal growth inside the plant, which was evident 5 days after inoculation with the mutant strain. By contrast, the delayed activation of plant defences in response to wild-type infection is not sufficient to prevent disease development. In addition, increased endochitinase activity was detected in plants either single or co-inoculated with the Δ*chsV* mutant. By contrast, no cell wall appositions or differential accumulation of reactive oxygen species were observed in response to the nonvirulent mutant infection. Alterations in the response to nonvirulent *Fusarium* isolates in comparison with virulent strains have been reported previously in other systems (van Kan *et al*., 1992). Plants inoculated with the nonvirulent strain Fo47 showed wall appositions and increased levels of PR-1 protein, chitinase, β-1,3-glucanase and β-1,4-glucosidase activities (Benhamou and Garand, 2001; Duijff *et al*., 1998; Fuchs *et al*., 1997; Olivain *et al*., 2003); plants treated with the nonvirulent *Fusarium* strain CS-20 showed increased accumulation of phenolic compounds (Panina *et al*., 2007). Attenuated expression of PR-5- and PR-7-encoding genes was detected in *F. solani* strain Fs-K-infected plants (Kavroulakis *et al*., 2007).

The elicitation of plant defence reactions has also been attributed to the secretion of increased amounts of CWDEs by the pathogen (Di Pietro *et al*., 2003). However, the Δ*chsV* mutant did not show the differential expression of several CWDE genes tested during plant infection, indicating that the cell wall rigidity defect has no pleiotropic effect on the expression of CWDEs.

In summary, we have demonstrated that the Δ*chsV* mutant, lacking a chitin synthase essential for pathogenicity, is able to penetrate tomato roots, grow efficiently inside plant cells and elicit the plant defence response. The activation of plant defences might be caused simply by the increased fungal biomass of the Δ*chsV* mutant within infected tissues. Presumably, elicitors are readily released from the altered cell wall of the mutant, rapidly alerting the plant to activate its defences, highlighting the importance of the fungal cell wall in the infection process. These elicitors are more abundant at higher inoculum concentrations, and thus the protective effect exerted by the mutant is more effective in these conditions. Furthermore, the rapid response caused by the nonvirulent Δ*chsV* mutant protects the plant against infection by the pathogenic wild-type strain. In addition, both strains probably compete for nutrients and/or plant tissues. In this sense, the higher colonization efficiency of the Δ*chsV* mutant at the beginning of the infection process could be considered as an advantage over the wild-type strain. Thus, we propose two successive or simultaneous mechanisms to explain the protective effect exerted by the Δ*chsV* mutant: elicitation of plant defence responses and competition for tissue colonization. Our results highlight the importance of deciphering the molecular dialogue between the plant and pathogen during the early stages of infection in order to understand the bases that govern fungal pathogenicity.

EXPERIMENTAL PROCEDURES

Fungal isolates and culture conditions

Fusarium oxysporum f. sp. *lycopersici* wild-type strain 4287 (race 2) was obtained from J. Tello, Universidad de Almería, Spain. The

Δ*chsV* mutant deficient in the class V chitin synthase gene (Madrid *et al*., 2003), the Δ*fmk1* mutant deficient in the mitogen-activated protein kinase 1 (Di Pietro *et al*., 2001), the Δ*gas1* mutant deficient in a β-1,3-glucanosyltransferase (Caracuel *et al*., 2005) and the wild-type harbouring histone H1 tagged with GFP (wild-type FoH1::GFP) (M. C. Ruiz-Roldán *et al*., unpublished) have been described elsewhere. Tagging of histone H1 in the Δ*chsV* mutant strain was completed by fusion PCR, as described previously (Yang *et al*., 2004), using a cassette containing a hinge region encoding five Gly-plus-Ala repeats in frame at the N-terminus of ChFP of mRFP (Campbell *et al*., 2002; Shaner *et al*., 2004), followed by the phleomycin resistance cassette as a selectable marker (M. C. Ruiz-Roldán *et al*., unpublished). The tagging construct was used to transform protoplasts of *F. oxysporum* f. sp. *lycopersici* isolate 4287, as reported previously (Di Pietro and Roncero, 1998). Several transformants carrying a copy of ChFP-tagged *hisH1* at the homologous locus (Δ*chsV*-FoH1::ChFP) were identified by PCR and southern hybridization. Tomato infection assays were performed using wild-type FoH1::GFP or Δ*chsV* FoH1::ChFP in order to confirm their pathotypic behaviour: highly virulent and nonvirulent, respectively (data not shown).

Microconidial suspensions were stored with 30% glycerol at −80 °C. The pathotype of the isolates was confirmed periodically by plant infection assays. For fungal DNA extraction and microconidia production, cultures were grown in potato dextrose broth (PDB) (Difco Laboratories, Detroit, MA, USA) at 28 °C with shaking at 170 rpm for 3 days, as described previously (Di Pietro and Roncero, 1998).

Plant infection

For pathogenicity assays, infection of tomato plants was performed as reported previously (Di Pietro and Roncero, 1998). Briefly, 2-week-old tomato seedlings were inoculated with *F. oxysporum* wild-type and/or mutant strains by immersing the roots in a suspension of 5×10^6 microconidia/mL (1 × concentration), 2.5×10^6 microconidia/mL (0.5 × concentration) or 5×10^5 microconidia/mL (0.1 × concentration) for 30 min. For co-inoculation experiments, microconidia of both strains were mixed at the desired concentrations. The inoculum size of each strain during co-inoculation is indicated as a ratio of wild-type : mutant strain. As controls, tomato roots were immersed in microconidial suspension from one strain for 15 min, followed by immersion in a suspension of the other strain during an additional 15 min. Infected tomato seedlings were planted in vermiculite and maintained in a growth chamber. Fifteen plants were used for each treatment. The severity of disease symptoms was recorded at different times after inoculation using the following index: 1, no apparent symptoms; 2, beginning of wilt symptoms in leaves; 3, leaves heavily wilted; 4, all leaves completely wilted; 5, dead plant (Huertas-Gonzalez *et al*., 1999). Virulence experiments were performed three times. Data were analysed with the software SPSS 15.0 for Windows® (LEAD Technologies, Inc., Charlotte, NC, USA). ANOVA was performed and the Duncan *post hoc* test was executed to assess the differences among treatments within each day at $P \leq 0.05$. The arcsine transformation was performed for data normalization. For fluorescence microscopy analysis, tomato roots were immersed in a microconidial suspension at the desired concentration for 30 min, planted in vermiculite and maintained in a growth chamber for 5 days.

For light microscopy, SEM and TEM, tomato roots were immersed in Erlenmeyer flasks containing a suspension of 5×10^6 spores/mL, and maintained in a growth chamber at 80 rpm. At different times after inoculation, 1-cm tissue sections were excised from three different root zones, the root tip, the middle root (around 3 cm away from the root tip) and the upper root (around 6 cm away from the root tip), and the samples were processed for further analysis.

Inoculations for the analysis of fungal colonization, plant defence-related gene expression and fungal gene expression were performed by immersing the roots in microconidial suspensions at the desired concentrations, and the flasks were maintained in a growth chamber at 80 rpm for 1, 3, 5 or 7 days. After incubation, roots and stems were collected separately and stored at −80 °C until analysis. Five plants were used per treatment.

Seeds from tomato cv. Abramo, Monika, Moneymaker and Vemar were kindly provided by Syngenta (Almeria, Spain).

Microscopy

Sections of infected roots were wetted with water and placed directly on glass slides to be observed using a Leica DMRB microscope (Leica Microsystems, Wetzlar, Germany) by the DIC technique. Fluorescence was obtained using appropriate filter blocks: GFP for green fluorescence (470/40-nm excitation, 500-nm dichromatic mirror, 525/50-nm barrier filter; Leica) or TX2 for red fluorescence (560/40-nm excitation, 595-nm dichromatic mirror, 645/75-nm barrier filter; Leica). Photographs were recorded with a Leica DC 300F digital camera. Dual colour images were acquired by sequential scanning with settings optimal for GFP, followed by settings optimal for ChFP. The projections of the individual channels were merged in Photoshop 7.0 (Adobe, San Jose, CA, USA) and ImageJ (National Institutes of Health, Bethesda, MA, USA) to facilitate visualization. For each treatment, an average of 10 sections from three different roots was examined. For SEM, 5-mm sections of infected roots were fixed for 2 h in 2% glutaraldehyde at room temperature and dehydrated through a graded ethanol series (30–100%) followed by 100% acetone for critical point drying. Samples were coated with a thin gold layer and observed with a JEOL

6300 scanning electron microscope. For each treatment, an average of 10 sections from three different roots was examined.

For TEM, 1-cm sections of infected roots were fixed overnight at 4 °C in a mixture of 2.5% glutaraldehyde and 2% paraformaldehyde in 0.1 M sodium cacodylate buffer pH 7.0 (CAB). After fixation, tissues were washed twice for 10 min in CAB and post-fixed for 45 min in 1% (v/v) osmium tetroxide in CAB. Tissues were then washed again in CAB (twice for 10 min) and dehydrated in a graded ethanol series [30, 50, 70, 80 and 90% (v/v) ethanol; 15 min each change and then three changes of 100% ethanol of 20 min each in duration]. Samples were transferred to two changes of propylene oxide of 20 min each in duration and progressively embedded in Epon 812 (Polaron, Watford, UK). Tissues were then subjected to 12 h in pure resin, followed by a change of fresh resin for 4 h, placed in blocks and polymerized at 65 °C for 48 h. Ultrathin sections (80 nm) were cut with a diamond knife and mounted on copper grids. The samples were stained in 2% aqueous uranyl acetate for 2 min at 37 °C, and then transferred to Reynold's lead citrate for 3 min at room temperature. Micrographs were obtained using a Philips CM 10 electron microscope (Cambridge, UK). For each treatment, an average of five samples from three different roots was investigated. For each sample, 10–15 ultrathin sections were examined.

Cytochemical detection of hydrogen peroxide (H_2O_2)

The histochemical method used for the localization of H_2O_2 was based on the generation of cerium perhydroxides described previously (Bestwick *et al*., 1997). One-centimetre sections were excised from roots 24 and 48 h post-inoculation. Noninoculated plants were included as controls. Sections were incubated in freshly prepared 5 mM $CeCl_3$ in 50 mM 3-(*N*-morpholino)propanesulphonic acid (MOPS) at pH 7.2 for 1 h at room temperature. Tissues were then fixed, post-fixed, dehydrated and embedded as described above for TEM. Unstained 80-nm sections were examined using a Philips CM 10 electron microscope. For each treatment, an average of five samples from three different roots was investigated. For each sample, 10–15 ultrathin sections were analysed.

Fungal inhibition assay

Inhibition assays in axenic cultures were performed by simultaneous inoculation of 2.5×10^5 spores/mL from both the wild-type FoH1::GFP strain harbouring the phleomycin resistant cassette and the Δ*chsV* mutant (resistant to hygromycin) into minimal medium (MM). Cultures were incubated at 28 °C with shaking at 170 rpm, and aliquots were removed 0, 2, 4, 6 or 8 h after inoculation, and plated on MM agar plates containing either 55 μg/mL hygromycin or 5.5 μg/mL phleomycin. Fungal inhibition was estimated by colony counting after 2 days at 28 °C. Control experiments were conducted by the single inoculation of either the wild-type FoH1::GFP strain or the Δ*chsV* mutant in MM. In addition, MM agar plates were inoculated with water droplets containing 10^3 spores from either the wild-type strain or the Δ*chsV* mutant. The colony diameter and distance between the colony margins were measured after incubation for 7 days at 28 °C. All experiments were performed three times.

Nucleic acid isolation

Total genomic DNA from mycelia was extracted from each strain and from stems of noninfected and infected plants using the commercially available DNeasy Plant Mini kit (Qiagen, Hilden, Germany) according to the manufacturer's instructions. Total RNA was isolated from germlings and from roots of noninfected and infected plants using the RNeasy Plant Mini Kit (Qiagen) according to the manufacturer's instructions. The quality of extracted nucleic acids was verified by running aliquots in ethidium bromide-stained agarose gels [0.7% w/v in Tris-acetate-EDTA (TAE) buffer] and further visualized under ultraviolet (UV) light. In addition, they were also quantified spectrophotometrically in a NanoDrop ND-1000 Spectrophotometer (NanoDrop Technologies, Wilmington, DE, USA). The isolated RNA was treated with deoxyribonuclease I (DNase I, Fermentas, Glen Burnie, MD, USA) and used to synthesize cDNA with the ribonuclease inhibitor RNasin Plus RNase Inhibitor (Promega, Madison, WI, USA) and M-MLV Reverse Transcriptase (Invitrogen, Carlsbad, CA, USA), according to the manufacturer's instructions, using a poly-dT antisense primer.

In planta quantification of *F. oxysporum* strains

Plant roots were maintained immersed in microconidial suspensions of the wild-type strain (5×10^5 microconidia/mL) and the Δ*chsV* mutant (5×10^6 microconidia/mL), either separately or simultaneously, for 3, 5 or 7 days. To avoid amplification of genomic DNA from external fungal mycelium which had not penetrated the roots, only the stems were collected for DNA analysis. Five plants were used per treatment. Real-time PCR assays for the quantification of fungal genomic DNA from infected stems were performed using primer pairs CHSV-3 (5′-ACAGCTCCAACGAACTCTCTT-3′) and CHSV-26 (5′-GGAGGTA CTTGGTCATGTCGT-3′) for specific detection of the wild-type strain (Madrid *et al*., 2003), and GPDA-16 (5′-AGGGGCT GTATTAGGTCTC-3′) and CHSV-6 (5′-CCGAGTTTCTGGGTAT GACA-3′) for specific detection of the Δ*chsV* mutant strain, which define amplicons of 511 and 460 bp, respectively. Primer specificity was corroborated by standard PCR using fungal genomic DNA from both strains as template (data not shown).

Reaction mixtures contained 12.5 μL of iQ SYBR Green Supermix (Bio-Rad, Hercules, CA, USA), 300 nM of each primer and

100 ng of total DNA extracted from stems in a final volume of 25 μL. Three simultaneous replicated amplifications were carried out for each DNA sample, using 25-μL aliquots from a 75-μL mixture. Amplification reactions were performed in 96-well microtitre plates (Bio-Rad). PCRs were performed in an iCycler apparatus (Bio-Rad) using the following cycling protocol: an initial step of denaturation (5 min, 94 °C) followed by 40 cycles of 30 s at 94 °C, 30 s at 62 °C for wild-type strain detection or 60 °C for Δ*chs*V strain detection, 45 s at 72 °C and 20 s at 80 °C for measurement of the fluorescence emission. After this, a melting curve programme was run for which measurements were made at 0.5 °C temperature increases every 5 s within a range of 55–95 °C. Finally, PCR products were also visualized under UV light in ethidium bromide-stained agarose gels (1% in TAE buffer).

The DNA concentration of each sample was extrapolated from standard curves, which were developed by plotting the logarithm of known concentrations (10-fold dilution series from 10 ng to 1 pg/25 μL reaction) of DNA from *F. oxysporum* strains against the Ct values. In order to normalize the amplification conditions of the serially diluted DNA samples, 100 ng of DNA from noninoculated plants were added to each sample in the dilution series. The experiment was repeated three times using independent infected tissues. Data were analysed with the software SPSS 15.0 for Windows® (LEAD Technologies, Inc.). ANOVA was performed and the Duncan *post hoc* test was executed to assess the differences among treatments within each day at $P \leq 0.05$.

Quantitative PCR of defence-related genes

Real-time PCRs were performed in an iCycler apparatus (Bio-Rad) using iQ SYBR Green Supermix (Bio-Rad), 2 μL of cDNA template and 300 nM of each gene-specific primer (Table S1, see Supporting Information) in a final reaction volume of 25 μL. All primer pairs amplified products of 160–200 bp. The following PCR programme was used for all reactions: an initial step of denaturation (5 min, 94 °C), followed by 40 cycles of 30 s at 94 °C, 30 s at 60 °C, 30 s at 72 °C and 20 s at 80 °C for measurement of the fluorescence emission. A melting curve programme was run for which measurements were made at 0.5 °C temperature increments every 5 s within a range of 55–95 °C. Each sample reaction was performed in duplicate for each gene assay. Relative levels of the RT-PCR products were determined using the ΔΔCt method (Livak and Schmittgen, 2001). Ct values were normalized to the Ct value of the *gapdh* housekeeping gene. Normalized transcript levels of each gene in infected samples were compared with levels in noninoculated samples. The experiments were repeated four times with independent infected tissues. Data were analysed with the software SPSS 15.0 for Windows® (LEAD Technologies, Inc.). ANOVA was performed and the Duncan *post hoc* test was executed to assess differences among treatments for each gene at $P \leq 0.05$.

RT-PCR analysis of fungal CWDE genes

To determine the expression of *Fusarium* genes encoding CWDEs, total RNA from roots obtained 1 or 3 days after inoculation, or from germlings grown for 14 h in PDB medium, was used as a template for RT-PCR. Specific primers were designed for each gene based on the predicted *F. oxysporum* f. sp. *lycopersici* protein sequences available at the Broad Institute database (Table S2, see Supporting Information). The *F. oxysporum actin 1* gene was used as a control for gene expression, and genomic DNA as control template for size comparison with bands amplified from cDNA of intron-containing genes. PCR products were electrophoretically separated in 2% agarose gels, stained with ethidium bromide and photographed. Assays were repeated in three independent experiments with similar results.

Detection of chitinase activity

Crude enzyme extracts were obtained from infected plant stems. Four plants per treatment were bulked prior to enzyme extraction. Stems were separated, washed under running water, dried gently and ground with a mortar and pestle under liquid nitrogen. Samples were homogenized in phosphate buffer (0.05 M, pH 6.0) by vortexing, followed by incubation at 4 °C for 2 min. The homogenate was centrifuged twice at 10 000 ***g*** and 4 °C, and the supernatant was collected and stored at −20 °C. The protein content was quantified according to the method of Bradford using the Bio-Rad protein assay (Bio-Rad, Munchen, Germany), with bovine serum albumin as standard. Endo- and exochitinase activities were measured using the Fluorimetric Chitinase Assay Kit (Sigma, Ronkonkoma, NY, USA) following the manufacturer's instructions. Chitinase activity is expressed as nanograms of 4-methylumbelliferone released from the substrate per microgram of protein. Assays were performed in three independent experiments, each including four plants per treatment. Data were analysed with the software SPSS 15.0 for Windows® (LEAD Technologies, Inc.). ANOVA was performed and the Duncan *post hoc* test was executed to assess differences among treatments at $P \leq 0.05$.

ACKNOWLEDGEMENTS

The authors gratefully acknowledge E. Martínez for technical assistance, Dr A. Muñoz for statistical analyses and Dr A. Di Pietro for critical reading of the manuscript, all from the University of Córdoba, Spain. This research was supported by the Ministerio de Educación y Ciencia of Spain (BIO2004-0276) and

Junta de Andalucía (CVI-138 and AGR-209). Y. Pareja-Jaime was supported by a fellowship from the Ministerio de Educación y Ciencia of Spain.

REFERENCES

Alabouvette, C., Olivain, C. and Steinberg, C. (2006) Biological control of plant diseases: the European situation. *Eur. J. Plant Pathol.* **114**, 329–341.

Alabouvette, C., Olivain, C., Migheli, Q. and Steinberg, C. (2009) Microbiological control of soil-borne phytopathogenic fungi with special emphasis on wilt-inducing *Fusarium oxysporum*. *New Phytol.* **184**, 529–544.

Armstrong, G.M. and Armstrong, J.K. (1981) Formae speciales and races of *Fusarium oxysporum* causing wilt diseases. In: *Fusarium: Disease, Biology, and Taxonomy* (Nelson, P.E., Tousson, T.A. and Cook, R.J., eds), pp. 391–399. University Park, PA: State University Press.

Benhamou, N. and Garand, C. (2001) Cytological analysis of defense-related mechanisms induced in pea root tissues in response to colonization by nonpathogenic *Fusarium oxysporum* Fo47. *Phytopathology*, **91**, 730–740.

Bestwick, C.S., Brown, I.R., Bennett, M.H.R. and Mansfield, J.W. (1997) Localization of hydrogen peroxide accumulation during the hypersensitive reaction of lettuce cells to *Pseudomonas syringae* pv *phaseolicola*. *Plant Cell*, **9**, 209–221.

Campbell, R.E., Tour, O., Palmer, A.E., Steinbach, P.A., Baird, G.S., Zacharias, D.A. and Tsien, R.Y. (2002)A monomeric red fluorescent protein. *Proc. Natl. Acad. Sci. USA*, **99**, 7877–7882.

Caracuel, Z., Martinez-Rocha, A.L., Di Pietro, A., Madrid, M.P. and Roncero, M.I.G. (2005) *Fusarium oxysporum gas1* encodes a putative β-1,3-glucanosyltransferase required for virulence on tomato plants. *Mol. Plant–Microbe Interact.* **18**, 1140–1147.

Dalisay, R.F. and Kuc, J.A. (1995) Persistence of induced resistance and enhanced peroxidase and chitinase activities in cucumber plants. *Physiol. Mol. Plant Pathol.* **47**, 315–327.

Danhash, N., Wagemakers, C.A., van Kan, J.A. and de Wit, P.J. (1993) Molecular characterization of four chitinase cDNAs obtained from *Cladosporium fulvum*-infected tomato. *Plant Mol. Biol.* **22**, 1017–1029.

Di Pietro, A. and Roncero, M.I.G. (1998) Cloning, expression, and role in pathogenicity of *pg1* encoding the major extracellular endopolygalacturonase of the vascular wilt pathogen *Fusarium oxysporum*. *Mol. Plant–Microbe. Interact.* **11**, 91–98.

Di Pietro, A., Garcia-Maceira, F.I., Meglecz, E. and Roncero, M.I.G. (2001) A MAP kinase of the vascular wilt fungus *Fusarium oxysporum* is essential for root penetration and pathogenesis. *Mol. Microbiol.* **39**, 1140–1152.

Di Pietro, A., Madrid, M.P., Caracuel, Z., Delgado-Jarana, J. and Roncero, M.I.G. (2003) *Fusarium oxysporum*: exploring the molecular arsenal of a vascular wilt fungus. *Mol. Plant Pathol.* **4**, 315–326.

Di Pietro, A., Roncero, M.I.G. and Ruiz-Roldan, M.C. (2009) From tools of survival to weapons of destruction: role of cell wall-degrading enzymes in plant infection. In: *The Mycota V: Plant Relationships* (Deising, H., ed.), pp. 181–200. Heidelberg, Berlin: Springer Verlag.

Duijff, B.J., Pouhair, D., Olivain, C., Alabouvette, C. and Lemanceau, P. (1998) Implication of systemic induced resistance in the suppression of fusarium wilt of tomato by *Pseudomonas fluorescens* WCS417r and by nonpathonic *Fusarium oxysporum* Fo47. *Eur. J. Plant Pathol.* **104**, 903–910.

Fravel, D., Olivain, C. and Alabouvette, C. (2002) *Fusarium oxysporum* and its biocontrol. *New Phytol.* **157**, 493–502.

Freeman, S. and Rodriguez, R.J. (1993) Genetic conversion of a fungal plant pathogen to a nonpathogenic, endophytic mutualist. *Science*, **260**, 75–78.

Freeman, S., Zveibil, A., Vintal, H. and Maymon, M. (2001) Isolation on nonpathogenic mutants of *Fusarium oxysporum* f. sp. *melonis* for biological control of Fusarium wilt in cucurbits. *Phytopathology*, **92**, 164–168.

Fuchs, J.-G., Moënne-Loccoz, Y. and Défago, G. (1997) Nonpathogenic *Fusarium oxysporum* strain Fo47 induces resistance to *Fusarium* wilt in tomato. *Plant Dis.* **81**, 492–496.

Heath, M.C. (1996) Plant resistance to fungi. *Can. J. Plant Pathol.* **18**, 469–475.

Hedley, P.E., Machray, G.C., Davies, H.V., Burch, L. and Waugh, R. (1994) Potato (*Solanum tuberosum*) invertase-encoding cDNAs and their differential expression. *Gene*, **145**, 211–214.

Huertas-Gonzalez, M.D., Ruiz-Roldan, M.C., Di Pietro, A. and Roncero, M.I.G. (1999) Cross protection provides evidence for race-specific avirulence factors in *Fusarium oxysporum*. *Physiol. Mol. Plant Pathol.* **54**, 63–72.

Kavroulakis, N., Ntougias, S., Zervakis, G.I., Ehaliotis, C., Haralampidis, K. and Papadopoulou, K.K. (2007) Role of ethylene in the protection of tomato plants against soil-borne fungal pathogens conferred by an endophytic *Fusarium solani* strain. *J. Exp. Bot.* **58**, 3853–3864.

Livak, K.J. and Schmittgen, T.D. (2001) Analysis of relative gene expression data using real-time quantitative PCR and the 2(–Delta Delta C(T)) method. *Methods*, **25**, 402–408.

Madrid, M.P., Di Pietro, A. and Roncero, M.I. (2003) Class V chitin synthase determines pathogenesis in the vascular wilt fungus *Fusarium oxysporum* and mediates resistance to plant defence compounds. *Mol. Microbiol.* **47**, 257–266.

Martin-Urdiroz, M., Roncero, M.I., Gonzalez-Reyes, J.A. and Ruiz-Roldan, C. (2008) ChsVb, a class VII chitin synthase involved in septation, is critical for pathogenicity in *Fusarium oxysporum*. *Eukaryot. Cell* **7**, 112–121.

Olivain, C., Trouvelot, S., Binet, M.N., Cordier, C., Pugin, A. and Alabouvette, C. (2003) Colonization of flax roots and early physiological responses of flax cells inoculated with pathogenic and nonpathogenic strains of *Fusarium oxysporum*. *Appl. Environ. Microbiol.* **69**, 5453–5462.

Panina, Y., Fravel, D.R., Baker, C.J. and Shcherbakova, L.A. (2007) Biocontrol and plant pathogenic *Fusarium oxysporum*-induced changes in phenolic compounds in tomato leaves and roots. *J. Phytopathol.* **155**, 475–481.

Postma, J. and Luttikholt, A.J.G. (1996) Colonization of carnation stems by a nonpathogenic isolate of *Fusarium oxysporum* and its effect on *Fusarium oxysporum* f. sp. *dianthi*. *Can. J. Bot.* **74**, 1841–1851.

Redman, R.S., Freeman, S., Clifton, D.R., Morrel, J., Brown, G. and Rodriguez, R.J. (1999a) Biochemical analysis of plant protection afforded by a nonpathogenic endophytic mutant of *Colletotrichum magna*. *Plant Physiol.* **119**, 795–804.

Redman, R.S., Ranson, J.C. and Rodriguez, R.J. (1999b) Conversion of the pathogenic fungus *Colletotrichum magna* to a nonpathogenic, endo-

phytic mutualist by gene disruption. *Mol. Plant–Microbe Interact.* **12**, 969–975.

Shaner, N.C., Campbell, R.E., Steinbach, P.A., Giepmans, B.N., Palmer, A.E. and Tsien, R.Y. (2004) Improved monomeric red, orange and yellow fluorescent proteins derived from *Discosoma* sp. red fluorescent protein. *Nat. Biotechnol.* **22**, 1567–1572.

Shih, M.C., Heinrich, P. and Goodman, H.M. (1991) Cloning and chromosomal mapping of nuclear genes encoding chloroplast and cytosolic glyceraldehyde-3-phosphate-dehydrogenase from *Arabidopsis thaliana*. Gene, **104**, 133–138.

Soulie, M.C., Perino, C., Piffeteau, A., Choquer, M., Malfatti, P., Cimerman, A., Kunz, C., Boccara, M. and Vidal-Cros, A. (2006) *Botrytis cinerea* virulence is drastically reduced after disruption of chitin synthase class III gene (*Bcchs3a*). *Cell. Microbiol.* **8**, 1310–1321.

van Kan, J.A., Joosten, M.H., Wagemakers, C.A., van den Berg-Velthuis, G.C. and de Wit, P.J. (1992) Differential accumulation of mRNAs encoding extracellular and intracellular PR proteins in tomato induced by virulent and avirulent races of *Cladosporium fulvum*. *Plant Mol. Biol.* **20**, 513–527.

Wattad, C., Freeman, S., Dinoor, A. and Prusky, D. (1995) A nonpathogenic mutant of *Colletotrichum magna* is deficient in extracellular secretion of pectate lyase. *Mol. Plant–Microbe Interact.* **8**, 621–626.

Weber, I., Assmann, D., Thines, E. and Steinberg, G. (2006) Polar localizing class V myosin chitin synthases are essential during early plant infection in the plant pathogenic fungus *Ustilago maydis*. *Plant Cell*, **18**, 225–242.

Werner, S., Sugui, J.A., Steinberg, G. and Deising, H.B. (2007) A chitin synthase with a myosin-like motor domain is essential for hyphal growth, appressorium differentiation, and pathogenicity of the maize anthracnose fungus *Colletotrichum graminicola*. *Mol. Plant–Microbe Interact.* **20**, 1555–1567.

Yang, L., Ukil, L., Osmani, A., Nahm, F., Davies, J., De Souza, C.P., Dou, X., Perez-Balaguer, A. and Osmani, S.A. (2004) Rapid production of gene replacement constructs and generation of a green fluorescent protein-tagged centromeric marker in *Aspergillus nidulans*. *Eukaryot. Cell*, **3**, 1359–1362.

SUPPORTING INFORMATION

Additional Supporting Information may be found in the online version of this article:

Fig. S1 Attachment of *Fusarium oxysporum* strains to tomato roots.

Fig. S2 Tomato roots inoculated with wild-type [harbouring green fluorescent protein (GFP)-tagged H1 histone, green] or Δ*chsV* mutant [harbouring cherry red fluorescent protein (ChFP)-tagged H1 histone, red].

Fig. S3 Expression pattern of *Fusarium oxysporum* cell wall-degrading enzyme coding genes during the infection of tomato plants with the wild-type strain, the Δ*chsV* mutant or with both strains simultaneously.

Table S1 Sequences of plant gene-specific primers used in quantitative polymerase chain reaction (PCR) expression analysis.

Table S2 Sequences of *Fusarium oxysporum* gene-specific primers used in reverse transcriptase-polymerase chain reaction (RT-PCR) expression analysis.

Please note: Wiley-Blackwell are not responsible for the content or functionality of any supporting materials supplied by the authors. Any queries (other than missing material) should be directed to the corresponding author for the article.

